Am J Transl Res 2022;14(9):6712-6725
www.ajtr.org /ISSN:1943-8141/AJTR0143951

Original Article

Transplantation of bFGF-transfected bone mesenchymal stem cells on collagen scaffolds promotes the regeneration of injured rat endometrium

Fang Chen[1*], Yingxin Gong[1,2*], Ninghong Jiang[1], Jingjing Xiao[1], Yaping Wang[1,2], Limei Chen[1], Long Sui[1]

[1]Department of Gynecology and Obstetrics, Obstetrics and Gynecology Hospital of Fudan University, Shanghai, China; [2]Shanghai Key Laboratory of Female Reproductive Endocrine Related Diseases, Shanghai, China. [*]Equal contributors.

Received May 6, 2022; Accepted August 12, 2022; Epub September 15, 2022; Published September 30, 2022

Abstract: Objective: This study aimed to verify the role of basic fibroblast growth factor (bFGF)-bone mesenchymal stem cells (BMSCs) loaded on collagen scaffolds for the repair of injured endometrium. Methods: We established an intrauterine adhesion (IUA) model in rats by endometrial resection and implanted BMSCs and bFGF-BMSCs loaded on collagen scaffolds into uteri. A total of 100 IUA model rats were divided into five groups: the control group, scaffold group, BMSC+scaffold group, vector-BMSC group, and bFGF-BMSC+scaffold group. The rats were sacrificed on the 3rd, 7th, 15th, and 45th days. The endometrium thickness, number of glands, and microvascular density were measured by hematoxylin and eosin staining, Masson staining, and immunohistochemistry staining of CD31. The expression of bFGF, vascular endothelial growth factor (VEGF), vimentin, and Ki67 was assayed by immunohistochemistry staining. Results: The bFGF-BMSCs loaded on the collagen scaffold significantly increased the endometrial thickness, gland number, and microvascular density, which greatly promoted the regeneration of the injured endometrium ($P<0.0001$). In addition, the expression levels of bFGF, VEGF, vimentin, and Ki67 were significantly higher in the bFGF-BMSC+scaffold group than in the BMSC+scaffold group ($P<0.05$). Conclusions: Our findings indicated that bFGF-BMSCs loaded on collagen scaffolds have the ability to prompt the regeneration of the endometrium after injury, contributing to a better understanding of stem cell treatment for intrauterine adhesion.

Keywords: Bone mesenchymal stem cells, intrauterine adhesion, basic fibroblast growth factor, collagen scaffold

Introduction

Intrauterine adhesion (IUA) is an aberrant adhesion within the uterus resulting from endometrial injury mainly caused by curettage after abortion, postpartum hemorrhage and hysteroscopic operation [1]. Women with IUA may suffer from infertility, chronic pelvic pain, and menstrual disorders. Current prevention and treatment for IUA include hyaluronan gel, intrauterine devices, Foley catheters, hysteroscopic excision, and stem cell therapy [2]. Stem cell treatment has been widely studied in animal models and small-scale clinical experiments. The treatment of stem cells, including human amniotic mesenchymal stromal cells (hAMSCs), menstrual blood-derived stromal cells (MbMSCs), umbilical cord-derived mesenchymal stromal cells (UCMSCs) and bone mesenchymal stem cells (BMSCs), showed effective potential to prompt the regeneration of the endometrium [3].

BMSCs possess high self-renewal and multidirectional differentiation ability and can differentiate into cartilage, adipose, endothelial and other tissues under cytokine induction and in different environments. Research on BMSCs is currently receiving attention in the field of stem cells due to their advantages of easy accessibility, exogenous gene compatibility, stemness stability, and low immunogenicity. BMSCs and BMSC-derived exosomes have been confirmed to play vital roles in the repair and reconstruction of injured tissues, such as improving angiogenesis and osteogenesis [4, 5]. The effect of BMSCs on the endometrium was first proven by Zhao et al., who revealed that the uterine infu-

sion of BMSCs improved endometrial thickness by modulating migration and immunomodulatory factors [6]. Reproductive advantages of BMSCs for IUA rats were further observed, and these partially resulted from the retrieval of leukemia inhibitory factor, the endometrial receptivity marker in the endometrial lining [7]. Vascular endothelial growth factor (VEGF)-modified BMSCs exhibited a better effect for thin endometrium than stem cell treatment alone [8]. Basic fibroblast growth factor (bFGF) cultivation increased the proliferative and clonogenic potential of mesenchymal stem cells [9], and bFGF-mesenchymal stromal cell (MSC) treatment improved the repair of arterial endothelial cells, skin and neurons [10-12]. However, the effect of bFGF-transfected BMSCs a vital factor modulating wound healing, on injured endometrium, has not been elucidated.

This study attempted to clarify the role of bFGF-BMSCs loaded on collagen scaffolds in the regeneration of injured endometrium and provide information for an auxiliary method for stem cell therapy. The study may contribute toward a better understanding of stem cell treatment for IUA.

Materials and methods

Animal and IUA modeling

All animals in this study were treated in accordance with the guidelines approved by the institutional ethics review board of the Obstetrics and Gynecology Hospital of Fudan University (Approval Number: Kyy2019-80). A total of 100 Sprague-Dawley (SD) rats aged 6-8 weeks were purchased from Silaike Corporation (Shanghai, China). The IUA rat model was established as previously described. Briefly, a 2.5 cm longitudinal abdominal incision was made after anesthesia and sterilization of the rat. Then, the Y-shaped uterus was isolated with caution, and the full-thickness endometrium was excised. After excision and hemostasis, the uterus was sutured and returned to the pelvic cavity. The 100 SD rats were classified into five groups: control group (IUA untreated), collagen scaffold group, BMSC+scaffold group, Vector (V)-BMSC group, and bFGF-BMSC+scaffold group.

Isolation, culture, and identification of BMSCs

Four-week-old female rats were sacrificed with diethyl ether. Both the femur and tibia were placed in sterile dishes and rinsed with phosphate-buffered saline (PBS). Then, the bone marrow was flushed from bone cavities with the hypoglycemic medium containing 10% fetal bovine serum (FBS), and a single-cell suspension was prepared after filtration with 200 μm cell strainers. After centrifugation and resuspension, the cells were seeded in culture flasks and incubated at 37°C in an atmosphere containing 5% carbon dioxide. Nonadherent cells and erythrocytes were removed after 24 hours of culture, and the fresh medium was added. The renewal of the culture medium was conducted every two to three days, and the passage was implemented when cells reached 80-90% confluence. Rat BMSCs of the third passage (P3) to the fifth passage (P5) were used in the subsequent experiment.

The BMSCs in P3 were digested with 0.05% trypsin-ethylenediaminetetraacetic acid (EDTA), centrifuged, and resuspended in 500 μl PBS to generate a single-cell suspension at a concentration of 10^5/ml. The cells were then incubated with 0.5 μl of fluorescein isothiocyanate (FITC)-labeled anti-rat CD45 (BD Biosciences, USA), FITC-labeled anti-rat CD90 (BD Biosciences, USA), or PE-labeled anti-rat CD29 (BD Biosciences, USA) at 37°C for 30 min in the dark and washed with PBS. Flow cytometry was applied to perform the cytometric analysis. The adipogenic, osteogenic, and chondrogenic differentiation of BMSCs was conducted by induction media.

Transfection of bFGF and CCK-8 assay

The bFGF-GV297 lentiviral vector was constructed and identified by PCR and agarose gel electrophoresis. BMSCs at the third passage were seeded in 96-well plates at a concentration of 2×10^4 cells/cm^2, transfected with lentivirus suspension in a multiplicity of infection (MOI) gradient (MOI15, MOI20, MOI25, and MOI30) and incubated at 37°C for 8 hours. The expression of fluorescence was captured by fluorescence microscopy 72 hours after transfection.

P3 and P5 bFGF-BMSCs were digested to prepare single-cell suspensions. BMSCs of the same passage were taken as the normal control group, and 3000 cells/well were inoculated in 96-well culture plates and incubated at 37°C in an incubator containing 5% CO_2. Each sample was quadrupled, and a blank control

was also set. Cell proliferation was detected by CCK8 assay at 24 h, 48 h, 72 h, and 96 h after seeding, and the absorbance was measured by an enzyme-linked immunosorbent assay at a wavelength of 450 nm.

Real-time polymerase chain reaction

Total RNA extraction was performed using TRIzol total RNA reagent (Beijing Tiangen Biotech, Co.). The reverse transcription reaction was completed using the RevertAid™ First Strand cDNA Synthesis Kit (Fermentas, Massachusetts, USA). Real-time PCR was performed with SYBR® Green Master Mix in an ABI PRISM® 7500 Sequence Detection System (Applied Biosystems Inc., Foster City, CA). The sequences of the primer pairs were as follows: bFGF, sense 5'-CTGCTGGCTTCTAAGTGTG-3', anti-sense 5'-CAACTGGAGTATTTCCGTG-3'; GAPDH, sense 5'-GCAGTGCCAGCCTCGTCTCATA-3', anti-sense 5'-TGTCACAAGAGAAGGCAGCCCT-3'. The thermal cycling parameters were initial denaturation at 95°C for 30 s, 40 cycles of amplifications at 95°C for 5 s, and 60°C for 20 s.

Western blotting

Total protein was extracted from the cultured BMSCs, and the concentration of bFGF was tested by western blotting. A certain amount of protein sample was mixed with loading buffer and separated by sodium dodecyl sulfate-polyacrylamide gel electrophoresis (SDS-PAGE) using a Bio-Rad electrophoresis and blotting system. Then, proteins of a certain molecular weight were transferred to polyvinylidene fluoride (PVDF) membranes. The membranes were blocked with 10% skim milk at room temperature for 1 hour and then incubated overnight at 4°C with the primary antibodies anti-bFGF (1:800; Cell Signaling Technology, USA) and anti-β-actin (1:1000; Cell Signaling Technology, USA). Then, the membranes were washed with TBST and incubated with horseradish peroxidase-conjugated secondary antibody for 1 hour at room temperature. The membranes were visualized by an enhanced chemiluminescence (ECL) system (ImageQuant LAS 4000, General Electric Company, Fairfield, CT, USA).

Preparation of collagen scaffolds

The collagen membranes were cut to a size of 2.5 × 0.5 cm^2 and placed in 12-well plates containing stem cell complete medium with the porous side up 30 min before inoculation and incubated at 37°C in a humidified incubator with 5% CO_2. The media was discarded before implantation, and the collagen membranes were dried with sterile absorbent paper. BMSCs in P3-P5 were suspended at a concentration of 3.5 × 10^7/ml, and 30 μl was added to the porous side of each collagen membrane. After incubating at 37°C for 1 hour to attach BMSCs, 1 ml of prewarmed fresh medium was added along the wall of the culture plate and incubated for 3-6 hours before transfer to the rat IUA model. The collagen membrane with its porous side was attached to the entire endometrium of the uterine cavity with sutures fixing the four ends of the membrane.

Histological analysis

The uteri were fixed in 4% paraformaldehyde for 24 hours and embedded in paraffin. The paraffin blocks were cut into 5-μm thick slices and attached to slides. Slides were deparaffinized and rehydrated and then stained with hematoxylin and eosin (H&E) (ab-245880, Abcam, Cambridge). For Masson staining, the slides were incubated with Masson staining mix for 5 min and then stained with aniline blue solution for 6.5 min. The area of collagen fibers stained blue relative to the total field of view was calculated using Image Pro-Plus 6.0. The endometrial thickness, number of glands, and vascular density in the transverse section of the uteri were counted under low magnification and analyzed with ImageJ software.

Immunohistochemistry

After deparaffinization, dehydration, and antigen retrieval, tissue sections were blocked with goat serum at room temperature for 1 hour and incubated overnight at 4°C with primary antibodies: anti-VEGF (ab2349, Abcam, Cambridge), anti-vimentin (ab8069, Abcam, Cambridge), and Ki67 (AB-9260, Millipore, Billerica). After being washed with PBS, the sections were incubated with secondary antibodies at room temperature for 1 hour. The slides were stained with 3,3-diaminobenzidine (DAB) at room temperature, lightly counterstained with hematoxylin, and dehydrated. Quantification of immunoreactivity was performed with Image Pro-Plus 6.0, and the mean optical density (MOD) was measured in 3-5 random fields of each slide.

Enzyme-linked immunosorbent assay (ELISA)

The supernatant of BMSCs was measured by a bFGF ELISA kit (ab246531, Abcam) following the manufacturer's protocol. All samples were tested in triplicate, and the results are presented as optical density (OD) values. The concentrations of bFGF were calculated by fitting the OD value-concentration linear curve made from the standard samples in the ELISA kit.

Statistical analysis

All data were analyzed by GraphPad Prism 9.0 and SPSS 22.0 software. The results are presented as the means ± SDs. The difference between two groups was measured by the independent-samples T test. The difference between multiple groups was measured by one-way analysis of variance (ANOVA) followed by Fisher's post-hoc test for multiple comparisons. $P<0.05$ was considered statistically significant.

Results

bFGF-BMSCs show characteristics of mesenchymal stem cells and multi-differentiation potential in vitro

The BMSCs and bFGF-BMSCs presented typical spindle morphology in vitro (**Figure 1A-D**). Flow cytometry was applied to identify the surface biomarkers of BMSCs (**Figure 1E-G**). The cytometric analysis showed that BMSCs highly expressed CD90 and CD29 but were scarce with CD45. The multi-differentiation assays confirmed the potential of bFGF-BMSCs to differentiate toward adipocytes, osteocytes, and chondrocytes (**Figure 1H-J**).

The expression of bFGF is stable and upregulated in bFGF-BMSCs

The bFGF-GV297 lentiviral vector was constructed and transfected into BMSCs. The expression of GFP was weak on the 3rd day after transfection and became stronger after proliferation and passage (**Figure 2A-C**). The expression proportions of GFP in the P3, P5, and P7 bFGF-BMSCs all exceeded 90%. The proliferation curves showed that the bFGF-BMSCs were more active than the BMSCs (**Figure 2D**). After 72 h, the growth of BMSCs in P3 and P5 began to slow down, while bFGF-BMSCs of the same passage were still in the logarithmic growth phase. The proliferation rate of BMSCs transfected with bFGF was faster than that of the control group during the whole cell growth cycle. In addition, the proliferation of bFGF-BMSCs accelerated with passage, represented by the higher perforation rate of P5 compared with P3, while it decelerated with passage in BMSCs.

Different MOIs of lentivirus were transfected into BMSCs, and the mRNA expression of bFGF in BMSCs transfected with each MOI was tested (**Figure 2E**). There were significant differences between the bFGF group and the control group ($P<0.0001$). The optimal MOI was 25. The upregulation of bFGF expression in bFGF-BMSCs compared with BMSCs was verified by Western blotting (**Figure 2F**). To detect the secretory function, the expression of bFGF in the supernatant was tested by ELISA (**Figure 2G**). The results showed significantly increased bFGF expression in bFGF-BMSCs compared with BMSCs ($P<0.0001$).

BMSCs can load onto the collagen membrane

The collagen membranes served as scaffolds to facilitate the maintenance of BMSCs in the uterus (**Figure 3A-C**). H&E staining visualized the growth condition of BMSCs implanted on the medium-treated collagen membrane. **Figure 3D-F** shows that most BMSCs adhered to the collagen scaffold in 3 hours, and the adhesion became firm after 24 hours with inward cellular growth. The collagen membrane was filled with many BMSCs 48 and 72 hours after implantation (**Figure 3G**, **3H**). Electron microscopy was applied to further examine the morphology of BMSCs after implantation into the collagen membrane. **Figure 3I-M** displays the consistent procedure of cellular adhesion with H&E staining images and further reveals that the morphology of BMSCs transformed from spherical to stretching deformation for better adhesion. The cells firmly combined with the collagen scaffolds and began to grow into collagen pores at 48 h and 72 h. The scaffolds were then inserted into the uteri as shown in **Figure 4A**. No obvious degeneration of the collagen scaffold was observed 3 days after post-operation, and uterine hydrops were observed in the uteri sampled on days 15 and 45 (**Figure 4B**). **Figure 4C** displays the fluorescent tracer images of BMSCs after transplantation. As

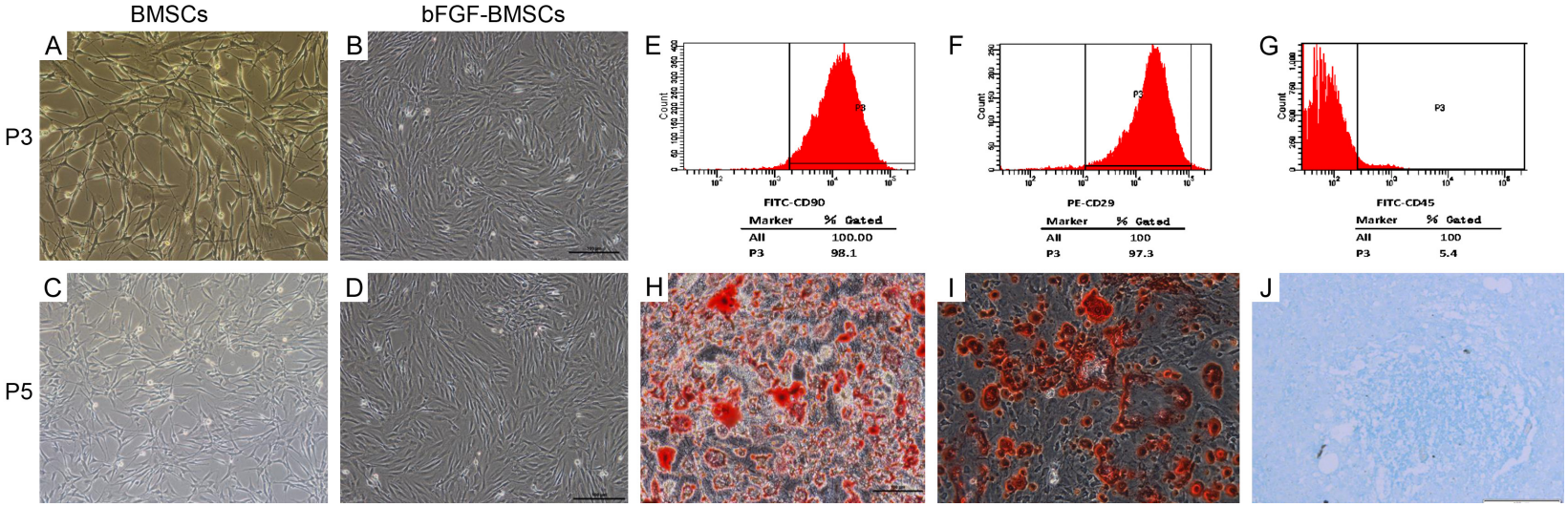

Figure 1. Identification of bone marrow stem cells in vitro. (A-D) Rat BMSCs and bFGF-BMSCs showed typical spindle fibroblast-like morphology at the 3rd and 5th passages. (E-G) The molecular markers on BMSCs were identified by flow cytometry, and the BMSCs were positive for CD90 (E) and CD29 (F) and negative for CD45 (G). (H-J) bFGF-BMSCs showed multidifferentiation potential in vitro. The cells displayed the abilityof BMSCs to differentiate into adipocytes (H, × 200), osteocytes (I, × 200) and chondrocytes (J, × 200).

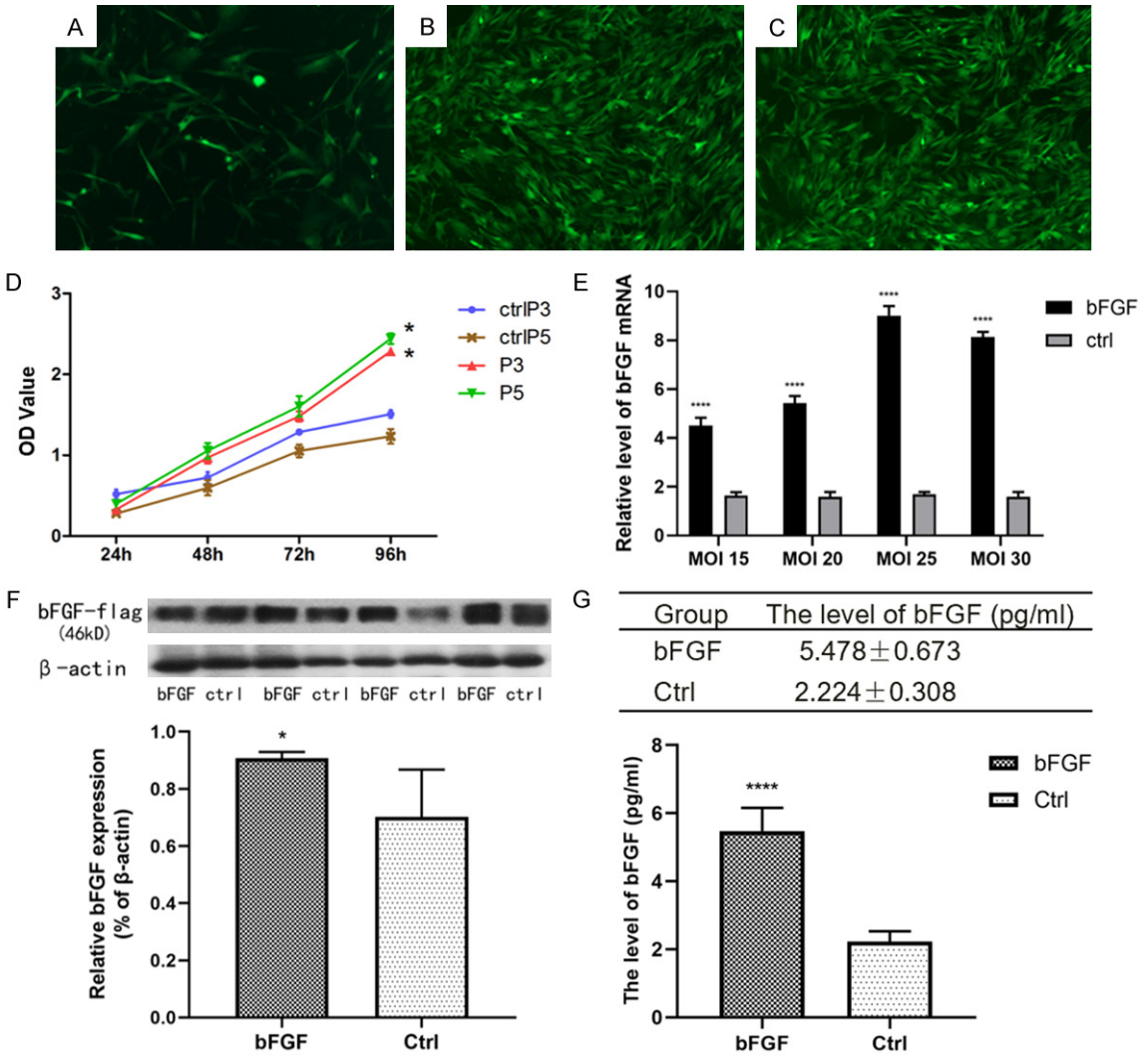

Figure 2. The expression of bFGF is stable and upregulated in bFGF-BMSCs. (A-C) The expression of bFGF was elevated in BMSCs after transfection with the EGFP-marked bFGF-GV287 lentiviral vector. The fluorescence expression was weak on the 3rd day after transfection (A) and increased in passages 3 (B) and 5 (C). (D) The proliferation curves of BMSCs tested by the CCK8 assay exhibited a faster proliferation rate in bFGF-transfected BMSCs than BMSCs. (E) The mRNA expression of bFGF in BMSCs transfected with lentivirus at different MOIs. (F) The expression of bFGF in BMSCs was significantly upregulated after transfection. (G) Expression of bFGF in the supernatant tested by ELISA. Note: *P<0.05; **P<0.01; ****P<0.0001.

shown in **Figure 4D**, the bFGF-BMSC+scaffold group displayed a slower fluorescence attenuation speed than the V-BMSC+scaffold group (P<0.0001). The expression of GFP was higher in the bFGF-BMSC+scaffold group than in the V-BMSC+scaffold group on both Day 7 and Day 45 after transplantation.

bFGF-BMSCs loaded on collagen scaffolds significantly promoted the repair of the injured endometrium

After the construction of the rat IUA model, the animals were divided into five groups: control (untreated group), scaffold, BMSC+scaffold, V-BMSC+scaffold, and bFGF-BMSCs+scaffold. Masson staining was used to evaluate the endometrial thickness and the number of glands in each group (**Figure 5A**). As shown in **Figure 5C**, the difference in endometrial thickness between the control group and scaffold group was not significant; this situation was also observed between the BMSC+scaffold group and the V-BMSC+scaffold group (P> 0.05). The endometrial thickness was different between the BMSC+scaffold group and scaffold group (P<0.0001), and it was thicker in the BMSC+scaffold group, with an average thick-

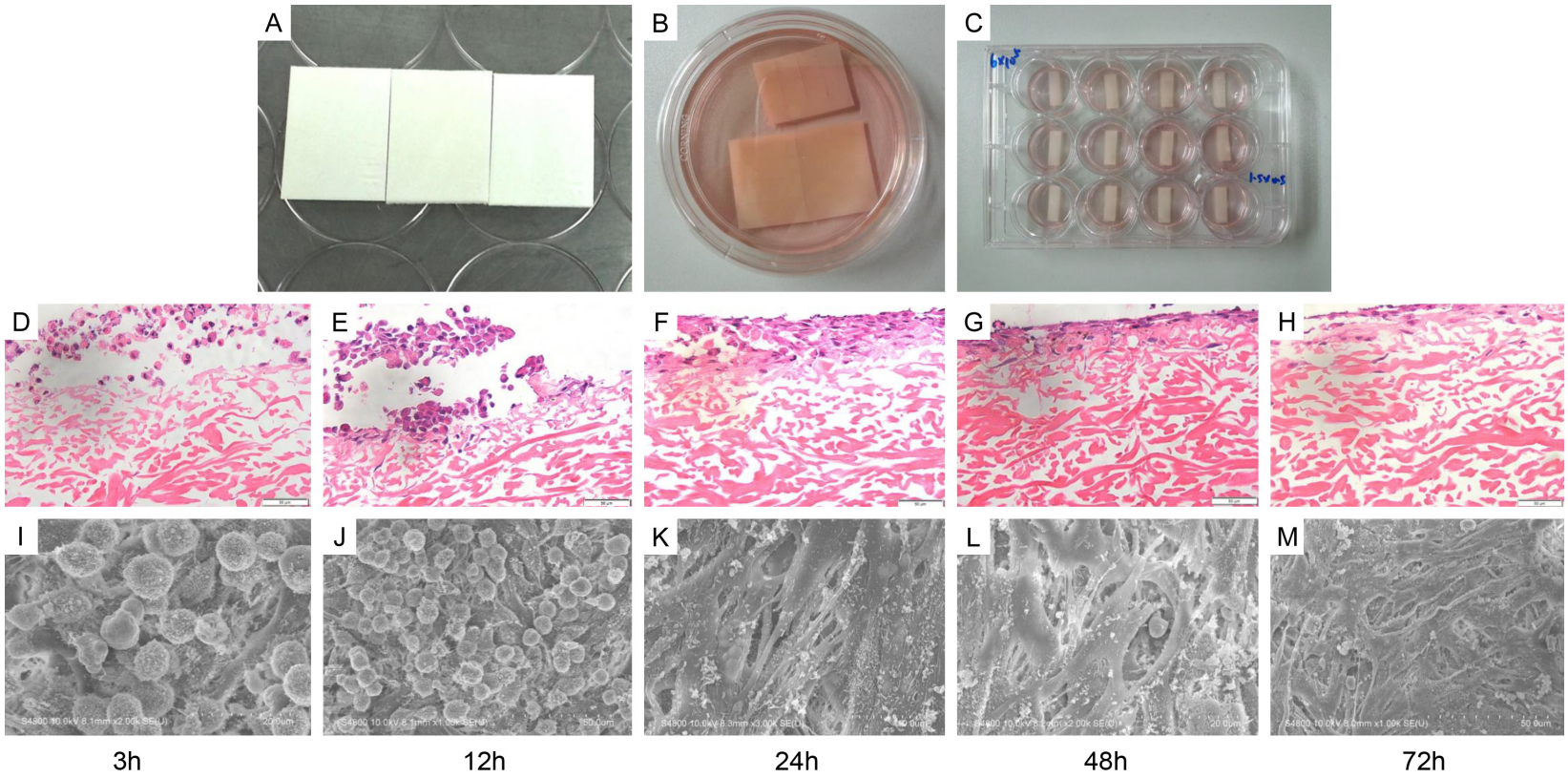

Figure 3. BMSCs can be loaded onto the collagen membrane. A-C. The collagen membranes were cut into 2.5 cm × 0.5 cm strips and dipped into complete medium with the porous side up for preparation. D-H. H&E staining images of collagen scaffolds loaded with BMSCs at different time points (3 h, 12 h, 24 h, 48 h, and 72 h). I-M. Electron microscopy was applied to further examine the morphology of BMSCs after implantation into the collagen membrane.

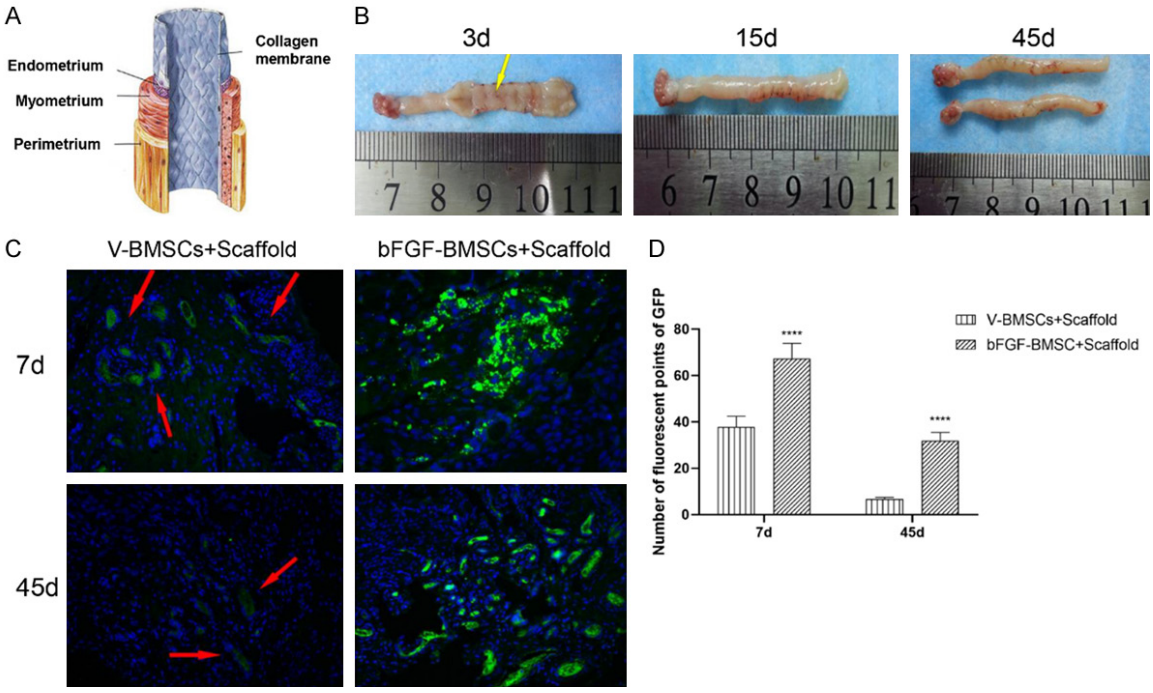

Figure 4. Implantation of the scaffold into the rat uterus. A. The model chart of in vivo implantation. The collagen membranes were tightly adhered to the endometrium. B. Gross observation of the uterus after collagen-borne stem cell transplantation. There was no obvious degradation of the collagen scaffold 3 days after transplantation, and uterine hydrops was observed in the uteri sampled 15 and 45 days postoperation. C. Fluorescence tracer images of BMSCs after transplantation. D. Number of fluorescent points of GFP in the endometrium after implantation. The expression of GFP was higher in the bFGF-BMSC+scaffold group than in the V-BMSC+scaffold group on both Day 7 and Day 45 (****P<0.0001).

ness of 360.61±60.34 μm. There was a significant difference between the bFGF-BMSC+ scaffold group and BMSC+scaffold group as well as between the bFGF-BMSC+scaffold group and scaffold+V-BMSC group (P<0.0001). The average thickness in the bFGF-BMSC+ scaffold group was 560.67±107.59 μm, which was the highest among the five groups. **Figure 5D** shows the growth of the glands over time. The bFGF-BMSC+scaffold group showed significant increases in the number of glands compared with the other groups on the 7th, 15th and 45th days after implantation (P<0.0001). There was no difference between the BMSC+scaffold and scaffold groups (P>0.05). CD31 immunohistochemistry was applied to visualize the microvessels (**Figure 5B**). The bFGF-BMSC+ scaffold group displayed the most apparent growth in microvascular density (MVD) compared with the other groups on the 7th, 15th and 45th days after implantation (P<0.0001). The differences among the BMSC+scaffold, V-BMSC+scaffold, scaffold, and control groups were not significant (P>0.05). All five groups presented significantly more glands and MVD on Day 45 than on Day 3 (**Figure 5E**).

bFGF-BMSCs loaded on collagen scaffolds significantly increase the expression of bFGF, VEGF, vimentin and Ki67

The immunohistochemistry staining of bFGF, VEGF, vimentin and Ki67 is visualized in **Figures 6A**, **6B** and **7A**, **7B**. As shown in **Figure 6C**, there were significant differences in bFGF expression between the bFGF-BMSC+scaffold group and the other four groups on the 7th, 15th and 45th days after implantation (P<0.0001). The expression of bFGF was greatly upregulated in the endometrium with BMSC implantation on the 15th day after transplantation. A difference was observed between the bFGF-BMSC+scaffold group and the BMSC+scaffold/V-BMSC+scaffold group (P<0.0001). No significant difference in bFGF expression was observed in any of the five groups between Day 45 and Day 15 (P>0.05). The expression of VEGF, vimentin and Ki67 was measured by

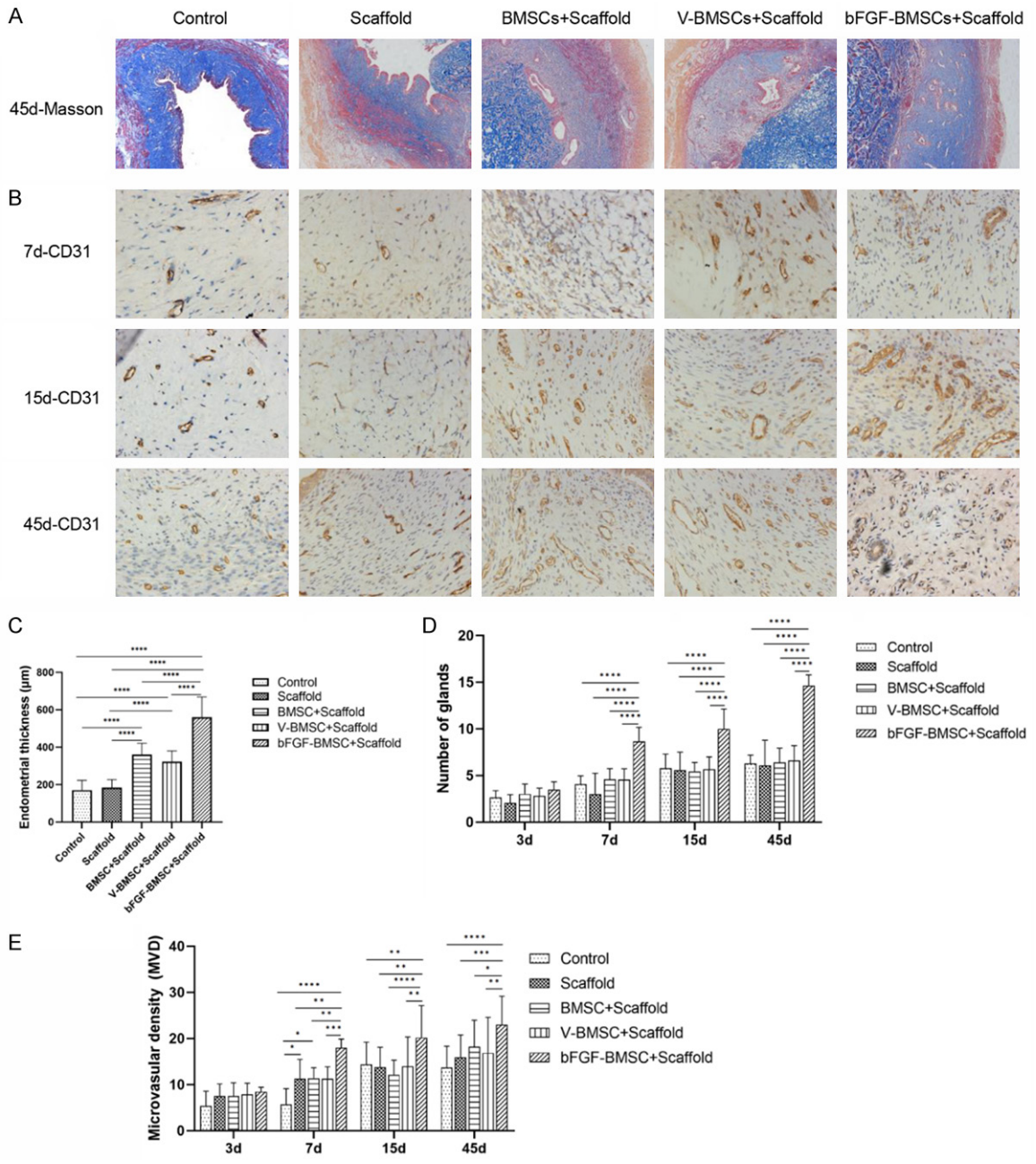

Figure 5. bFGF-BMSCs loaded on collagen scaffolds prompt the recovery of the injured endometrium. A. The morphology of the endometrium under Masson staining of the five groups on Day 45 postoperation. B. The expression of CD31 in the five groups under immunohistochemistry 7, 14 and 45 days after transplantation. C. Endometrial thickness of the five groups on the 45th day after the operation. D. The number of glands of the five groups 3, 7, 15 and 45 days after transplantation. E. The microvascular density of the five groups 3, 7, 15 and 45 days after transplantation. Note: *P<0.05; **P<0.01; ***P<0.001; ****P<0.0001.

immunohistochemical staining to further manifest the mechanism behind the role of bFGF-BMSCs in endometrial regeneration. **Figure 6D** shows the significantly high expression of VEGF in the bFGF-BMSC+scaffold group (P<0.01). The variable relationship between the bFGF-BMSC+scaffold group and the BMSC+scaffold/V-BMSC+scaffold group was also revealed. The difference between them was significant on the 15th day after transplantation (P<0.0001), whereas it was not significant on the 7th and 45th days (P>0.05). There was no difference in VEGF expression between the BMSC+scaffold/V-BMSC+scaffold group and

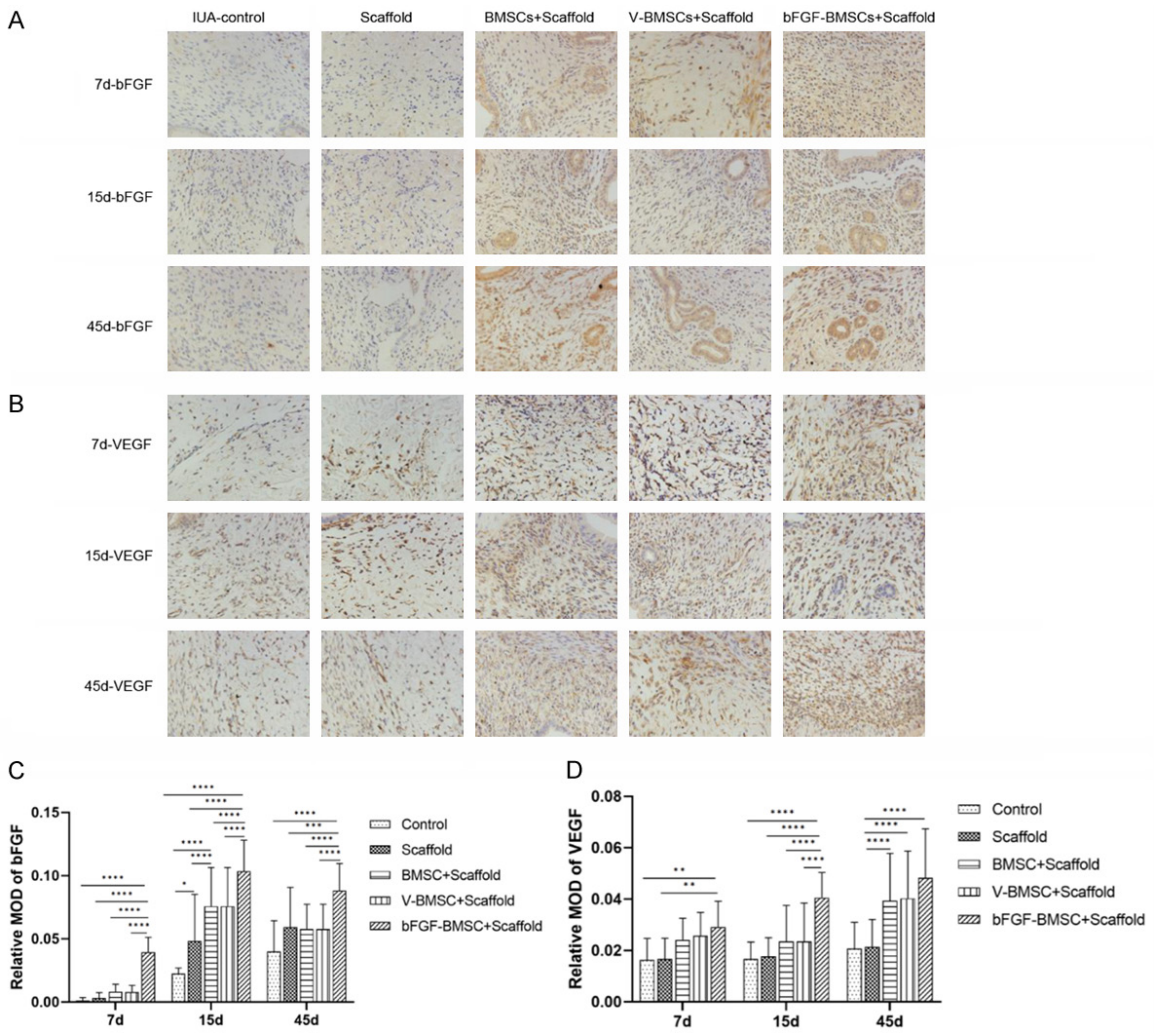

Figure 6. bFGF-BMSCs loaded on collagen scaffolds significantly increased the expression of bFGF and VEGF. A. Immunohistochemical staining of bFGF in the endometrium 7, 15 and 45 days after transplantation. B. Immunohistochemical staining of VEGF in the endometrium 7, 15 and 45 days after transplantation. C. The expression of bFGF was significantly upregulated after bFGF transfection. D. The expression of VEGF significantly increased in the bFGF-BMSC+scaffold group. Note: *P<0.05; **P<0.01; ***P<0.001; ****P<0.0001.

the control/scaffold group on Day 7 and Day 15 (P<0.05), while a significant difference was observed between the groups on Day 30 (P<0.0001). The expression of vimentin increased with time after implantation in all groups, and it reached the highest level in the bFGF-BMSC+scaffold group among the five groups on Day 45 (**Figure 7C**). No difference among the five groups was captured on the 7th day (P>0.05). The difference was significant between the bFGF-BMSC+scaffold group and BMSC+scaffold/V-BMSC+scaffold group (P<0.05) as well as between the BMSC+scaffold/V-BMSC+scaffold group and control/scaffold group (P<0.01) on the 15th and 45th days. Unlike vimentin, the expression of Ki67 displayed a significant downward trend with time from the 15th day after implantation (**Figure 7D**). The expression of Ki67 was significantly higher in the groups with BMSC implantation than in the control group and scaffold group (P<0.0001). Therefore, its expression in the bFGF-BMSC+scaffold group was significantly upregulated compared with its expression in the other two groups (P<0.0001).

Discussion

In this study, we isolated BMSCs from rats and constructed bFGF-BMSCs by lentivirus-mediated transfection in vitro. We established an IUA rat model by endometrial resection and transplanted BMSCs into the endometrium via the

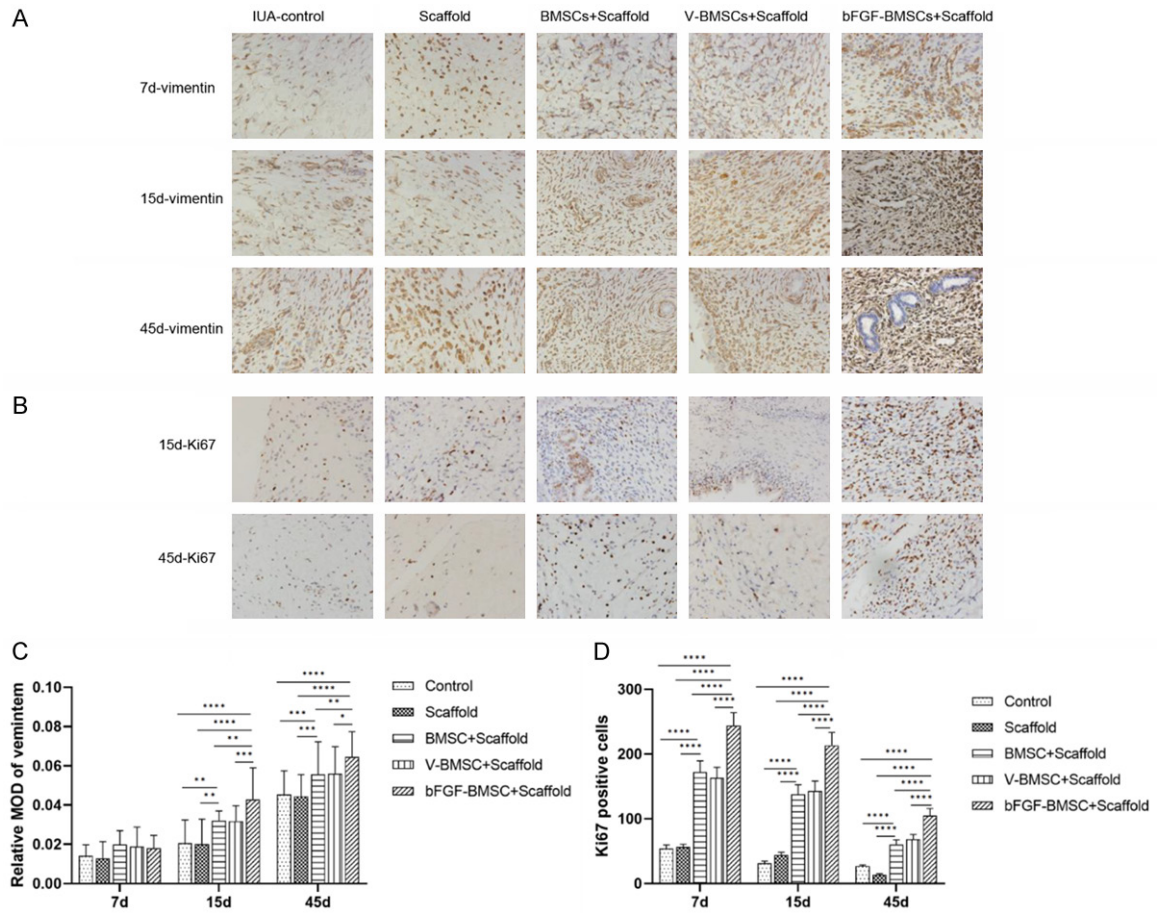

Figure 7. bFGF-BMSCs loaded on collagen scaffolds significantly increased the expression of vimentin and Ki67. A. Immunohistochemical staining of vimentin for endometrial stromal cell proliferation 7, 15 and 45 days after transplantation. B. Immunohistochemical staining of Ki67 for cell proliferation 15 and 45 days after transplantation. C. The expression of vimentin increased on the 15th and 45th days after BMSC transfection. D. The number of Ki67-positive cells significantly increased in groups transplanted with BMSCs. Note: *P<0.05; **P<0.01; ***P<0.001; ****P<0.0001.

collagen scaffold. Our results revealed that BMSCs loaded with collagen scaffolds prompted the regeneration of the endometrium injured by mechanical damage, and the promotion was most significant by bFGF-BMSCs.

Intrauterine adhesion is characterized by the loss of endometrial morphology and endometrial fibrosis. Endometrial injury, including iatrogenic damage such as dilation and curettage and hysteroscopic operation, can lead to IUA [13]. Various methods have been used to establish animal IUA models, including physical, chemical and mechanical injury [14, 15]. In this study, we used a mechanical injury to establish the IUA model, and the modeling was completed by the same researcher to minimize the bias between individuals. Stem cells present great therapeutic potential in the repair and regeneration of injured tissues. Previous studies revealed that uterine transplantation of BMSCs improved endometrial thickness and reproductive outcomes [6, 7]. In addition, various publications identified that extra measurements auxiliary to BMSCs, including scaffolds, platelet-rich plasma therapy, vitamin C plus hydrogel, and electroacupuncture, facilitated the regeneration of injured endometrium [16-19]. Transfection with the exogenous gene VEGF also provided an extra therapeutic advantage for BMSCs [8]. As in our previous study, bFGF was transfected into stem cells to promote survival and regeneration properties [20]. Overexpression of bFGF mRNA was observed after transfection, while the expression of bFGF protein in bFGF-BMSCs showed only slight upregulation. To further elucidate this finding, we conducted ELISA to detect the level of

secreted bFGF in the supernatant. The level of bFGF in the cell supernatant was significantly higher after transfection. The analysis of secreted bFGF confirmed its overexpression after transfection. It also revealed that bFGF exerted its role through the secretory form. A temporary suppression of cellular proliferation after transfection was also observed in this study, paralleling previous work. The toxic effect of the lentivirus might explain this phenomenon, as noted by Zhang et al. [21]. The proliferation promotion effect of bFGF greatly prompted rapid proliferation 10-12 days after transfection. The role of collagen scaffolds in allogeneic cell therapy has been extensively studied for their advantages in attachment to and maintenance of stem cells [20, 22, 23]. Our study revealed that the BMSCs adhered to the collagen membrane and infiltrated into the collagen pores, indicating the capability and stability of BMSCs for loading onto collagen scaffolds. A study compared the effects on damaged endometrium among BMSCs loaded on scaffolds of different materials and found that the poly(glycerol sebacate) (PGS) scaffold had superiority in morphology recovery but no advantage in fertility over the collagen scaffold [16]. The collagen membrane still serves as the most extensively used material for scaffolds, and phase I clinical trials have confirmed the safety and effectiveness of UCMSCs on collagen scaffolds in patients with recurrent IUAs [24].

Closer examination of endometrial thickness, gland number and microvascular density revealed that BMSCs loaded on collagen scaffolds significantly promoted the regeneration of mechanically injured endometrium. However, the endometrium with non-bFGF-transfected BMSC implantation did not display a significant increase in gland number or MVD compared with the control in our study. By analyzing the difference among groups implanted with bFGF-BMSCs, V-BMSCs and BMSCs, we deduced that bFGF transfection greatly facilitated endometrial repair. The bFGF is the primary promoter for cell proliferation and prompt migration, differentiation and angiogenesis [25, 26]. After binding to the FGF receptor, the downstream pathways are activated and regulate the process of inflammation, repair and regeneration [27, 28]. The roles of bFGF have been indicated in wound healing and regeneration [25, 29]. It also acts as a tumor promoter, possessing anti-apoptosis properties and prompting migration and differentiation [30, 31]. The expression of bFGF in the endometrium among the five groups was parallel to endometrial regeneration. The result confirmed the proliferation promotion effect of bFGF on injured endometrium, which was also proven in a study applying collagen-binding bFGF to the scarred endometrium of 20 women [32].

To better understand the mechanism behind the regeneration of the endometrium, the expression of cellular skeleton proteins and proliferation factors was evaluated. Previous research demonstrated elevated expression of vimentin, cytokeratin and anti-inflammatory cytokines, including bFGF and IL-6, in BMSC-treated endometria [33]. The expression of vimentin and Ki67 was upregulated in endometrium implanted with BMSCs and significantly increased in bFGF-BMSC-treated uteri. Considering the consistent expression pattern of vimentin and Ki67 with bFGF and endometrial regeneration, we speculated that bFGF prompted the regeneration of the endometrium by upregulating vimentin and Ki67. VEGF is a key factor in angiogenesis, and its expression was upregulated in the BMSC-treated endometrium, consistent with a previous study [16]. The expression of VEGF increased with time, which was consistent with the upward trend of MVD. However, the immunohistochemical results of bFGF-BMSC-treated endometrium only showed a significantly elevated level of VEGF compared with the BMSC-treated endometrium on the 14th day after implantation. The situation can be explained after referring to the less differentiated MVD between bFGF-BMSC- and BMSC-treated endometria on Day 45. In addition, the expression of bFGF did not parallel VEGF expression from the 15th day to the 30th day, suggesting that the expression of VEGF might not be completely regulated by bFGF despite the consistent overall trend in our study. In addition, bFGF-induced VEGF expression was observed in bFGF-human gingival MSCs, while the effect of VEGF on FGF expression was not observed in VEFG-MSCs liver transplantation [34, 35]. These findings suggested that bFGF-MSCs possess more regenerative potential than VEGF-MSCs.

The current study reveals the potential of bFGF-BMSCs loaded on collagen scaffolds for the regeneration of injured endometrium. However,

there were also some limitations. First, the study focused on the regeneration of the endometrium, including endometrial thickness, gland number and microvascular density, but the safety of the treatment was not clear. Second, the implantation method that used sutures fixing the four ends of the collagen membrane is not practicable for clinical use. Despite the meritorious findings, more work is needed before clinical application.

In light of our findings, it is reasonable to conclude that BMSCs loaded on collagen scaffolds have the potential to promote the proliferation of the endometrium, endometrial glands, and microvessels. The role of bFGF-BMSCs in endometrial regeneration was also identified. Further investigation of the safety and application of bFGF-BMSCs is needed.

Acknowledgements

We acknowledge the Shanghai Key Laboratory of Female Reproductive Endocrine Related Diseases. This work was funded by the Science and Technology Commission of Shanghai Municipality (No. 22ZR1408800).

Disclosure of conflict of interest

None.

Address correspondence to: Long Sui, Obstetrics and Gynecology Hospital of Fudan University, 419 Fangxie Road, Shanghai 200011, China. E-mail: suilong@fudan.edu.cn

References

[1] Salazar CA, Isaacson K and Morris S. A comprehensive review of Asherman's syndrome: causes, symptoms and treatment options. Curr Opin Obstet Gynecol 2017; 29: 249-256.

[2] Dreisler E and Kjer JJ. Asherman's syndrome: current perspectives on diagnosis and management. Int J Womens Health 2019; 11: 191-198.

[3] Song YT, Liu PC, Tan J, Zou CY, Li QJ, Li-Ling J and Xie HQ. Stem cell-based therapy for ameliorating intrauterine adhesion and endometrium injury. Stem Cell Res Ther 2021; 12: 556.

[4] Lu GD, Cheng P, Liu T and Wang Z. BMSC-derived exosomal miR-29a promotes angiogenesis and osteogenesis. Front Cell Dev Biol 2020; 8: 608521.

[5] Mao GC, Gong CC, Wang Z, Sun MX, Pei ZP, Meng WQ, Cen JF, He XW, Lu Y, Xu QQ and Xiao K. BMSC-derived exosomes ameliorate sulfur mustard-induced acute lung injury by regulating the GPRC5A-YAP axis. Acta Pharmacol Sin 2021; 42: 2082-2093.

[6] Zhao J, Zhang Q, Wang Y and Li Y. Uterine infusion with bone marrow mesenchymal stem cells improves endometrium thickness in a rat model of thin endometrium. Reprod Sci 2015; 22: 181-188.

[7] Gao L, Huang Z, Lin H, Tian Y, Li P and Lin S. Bone marrow mesenchymal stem cells (BMSCs) restore functional endometrium in the rat model for severe asherman syndrome. Reprod Sci 2019; 26: 436-444.

[8] Jing Z, Yi Y, Xi H, Sun LQ and Yanping L. Therapeutic effects of VEGF gene-transfected BMSCs transplantation on thin endometrium in the rat model. Stem Cells Int 2018; 2018: 3069741.

[9] Jauković A, Kukolj T, Trivanović D, Okić-Đorđević I, Obradović H, Miletić M, Petrović V, Mojsilović S and Bugarski D. Modulating stemness of mesenchymal stem cells from exfoliated deciduous and permanent teeth by IL-17 and bFGF. J Cell Physiol 2021; 236: 7322-7341.

[10] Wang P, Li J, Zhang C, Luo L, Ni S and Tang Z. bFGF overexpression adipose derived mesenchymal stem cells improved the survival of pulmonary arterial endothelial cells via PI3k/Akt signaling pathway. Int J Biochem Cell Biol 2019; 113: 87-94.

[11] Xu Z, Cao J, Zhao Z, Qiao Y, Liu X, Zhong J, Wang B and Suo G. A functional extracellular matrix biomaterial enriched with VEGFA and bFGF as vehicle of human umbilical cord mesenchymal stem cells in skin wound healing. Biomed Mater 2021; 17.

[12] Huang F, Gao T, Wang W, Wang L, Xie Y, Tai C, Liu S, Cui Y and Wang B. Engineered basic fibroblast growth factor-overexpressing human umbilical cord-derived mesenchymal stem cells improve the proliferation and neuronal differentiation of endogenous neural stem cells and functional recovery of spinal cord injury by activating the PI3K-Akt-GSK-3β signaling pathway. Stem Cell Res Ther 2021; 12: 468.

[13] Abudukeyoumu A, Li MQ and Xie F. Transforming growth factor-β1 in intrauterine adhesion. Am J Reprod Immunol 2020; 84: e13262.

[14] Zhang S, Sun Y, Jiang D, Chen T, Liu R, Li X, Lu Y, Qiao L, Pan Y, Liu Y and Lin J. Construction and optimization of an endometrial injury model in mice by transcervical ethanol perfusion. Reprod Sci 2021; 28: 693-702.

[15] Sun L, Zhang S, Chang Q and Tan J. Establishment and comparison of different intrauterine adhesion modelling procedures in rats. Reprod Fertil Dev 2019; [Epub ahead of print].

[16] Xiao B, Yang W, Lei D, Huang J, Yin Y, Zhu Y, You Z, Wang F and Sun S. PGS scaffolds promote

the in vivo survival and directional differentiation of bone marrow mesenchymal stem cells restoring the morphology and function of wounded rat uterus. Adv Healthc Mater 2019; 8: e1801455.
[17] Yang H, Wu S, Feng R, Huang J, Liu L, Liu F and Chen Y. Vitamin C plus hydrogel facilitates bone marrow stromal cell-mediated endometrium regeneration in rats. Stem Cell Res Ther 2017; 8: 267.
[18] Xia L, Meng Q, Xi J, Han Q, Cheng J, Shen J, Xia Y and Shi L. The synergistic effect of electroacupuncture and bone mesenchymal stem cell transplantation on repairing thin endometrial injury in rats. Stem Cell Res Ther 2019; 10: 244.
[19] Zhou Y, Shen H, Wu Y, Zhao X, Pei J, Mou Z, Dong J and Hua X. Platelet-rich plasma therapy enhances the beneficial effect of bone marrow stem cell transplant on endometrial regeneration. Front Cell Dev Biol 2020; 8: 52.
[20] Chen L, Guo L, Chen F, Xie Y, Zhang H, Quan P and Sui L. Transplantation of menstrual blood-derived mesenchymal stem cells (MbMSCs) promotes the regeneration of mechanical injuried endometrium. Am J Transl Res 2020; 12: 4941-4954.
[21] Zhang F, Peng WX, Wang L, Zhang J, Dong WT, Wu JH, Zhang H, Wang JB and Zhao Y. Role of FGF-2 transfected bone marrow mesenchymal stem cells in engineered bone tissue for repair of avascular necrosis of femoral head in rabbits. Cell Physiol Biochem 2018; 48: 773-784.
[22] Hu X, Dai Z, Pan R, Zhang Y, Liu L, Wang Y, Chen X, Yao D, Hong M and Liu C. Long-term transplantation human menstrual blood mesenchymal stem cell loaded collagen scaffolds repair endometrium histological injury. Reprod Toxicol 2022; 109: 53-60.
[23] Ebrahim N, Mostafa O, El Dosoky RE, Ahmed IA, Saad AS, Mostafa A, Sabry D, Ibrahim KA and Farid AS. Human mesenchymal stem cell-derived extracellular vesicles/estrogen combined therapy safely ameliorates experimentally induced intrauterine adhesions in a female rat model. Stem Cell Res Ther 2018; 9: 175.
[24] Cao Y, Sun H, Zhu H, Zhu X, Tang X, Yan G, Wang J, Bai D, Wang J, Wang L, Zhou Q, Wang H, Dai C, Ding L, Xu B, Zhou Y, Hao J, Dai J and Hu Y. Allogeneic cell therapy using umbilical cord MSCs on collagen scaffolds for patients with recurrent uterine adhesion: a phase I clinical trial. Stem Cell Res Ther 2018; 9: 192.
[25] Zhang X, Kang X, Jin L, Bai J, Liu W and Wang Z. Stimulation of wound healing using bioinspired hydrogels with basic fibroblast growth factor (bFGF). Int J Nanomedicine 2018; 13: 3897-3906.
[26] Kreuger J, Salmivirta M, Sturiale L, Giménez-Gallego G and Lindahl U. Sequence analysis of heparan sulfate epitopes with graded affinities for fibroblast growth factors 1 and 2. J Biol Chem 2001; 276: 30744-30752.
[27] Powers CJ, McLeskey SW and Wellstein A. Fibroblast growth factors, their receptors and signaling. Endocr Relat Cancer 2000; 7: 165-197.
[28] Barrientos S, Stojadinovic O, Golinko MS, Brem H and Tomic-Canic M. Growth factors and cytokines in wound healing. Wound Repair Regen 2008; 16: 585-601.
[29] Guan D, Mi J, Chen X, Wu Y, Yao Y, Wang L, Xiao Z, Zhao Y, Chen B and Dai J. Lung endothelial cell-targeted peptide-guided bFGF promotes the regeneration after radiation induced lung injury. Biomaterials 2018; 184: 10-19.
[30] Yang X, Hao J, Mao Y, Jin ZQ, Cao R, Zhu CH, Liu XH, Liu C, Ding XL, Wang XD, Chen D and Wu XZ. bFGF promotes migration and induces cancer-associated fibroblast differentiation of mouse bone mesenchymal stem cells to promote tumor growth. Stem Cells Dev 2016; 25: 1629-1639.
[31] Peluso JJ. Basic fibroblast growth factor (bFGF) regulation of the plasma membrane calcium ATPase (PMCA) as part of an anti-apoptotic mechanism of action. Biochem Pharmacol 2003; 66: 1363-1369.
[32] Jiang P, Tang X, Wang H, Dai C, Su J, Zhu H, Song M, Liu J, Nan Z, Ru T, Li Y, Wang J, Yang J, Chen B, Dai J and Hu Y. Collagen-binding basic fibroblast growth factor improves functional remodeling of scarred endometrium in uterine infertile women: a pilot study. Sci China Life Sci 2019; 62: 1617-1629.
[33] Jing Z, Qiong Z, Yonggang W and Yanping L. Rat bone marrow mesenchymal stem cells improve regeneration of thin endometrium in rat. Fertil Steril 2014; 101: 587-594.
[34] Adas G, Koc B, Adas M, Duruksu G, Subasi C, Kemik O, Kemik A, Sakiz D, Kalayci M, Purisa S, Unal S and Karaoz E. Effects of mesenchymal stem cells and VEGF on liver regeneration following major resection. Langenbecks Arch Surg 2016; 401: 725-740.
[35] Jin S, Yang C, Huang J, Liu L, Zhang Y, Li S, Zhang L, Sun Q and Yang P. Conditioned medium derived from FGF-2-modified GMSCs enhances migration and angiogenesis of human umbilical vein endothelial cells. Stem Cell Res Ther 2020; 11: 68.